Dynamic FRET: an avenue towards understanding biological macromolecules in motion

Maarten S. Overgaauw, supervision by Jaap Broos

Laboratory of Biophysical Chemistry, Department of Protein Crystallography, University of Groningen, the Netherlands

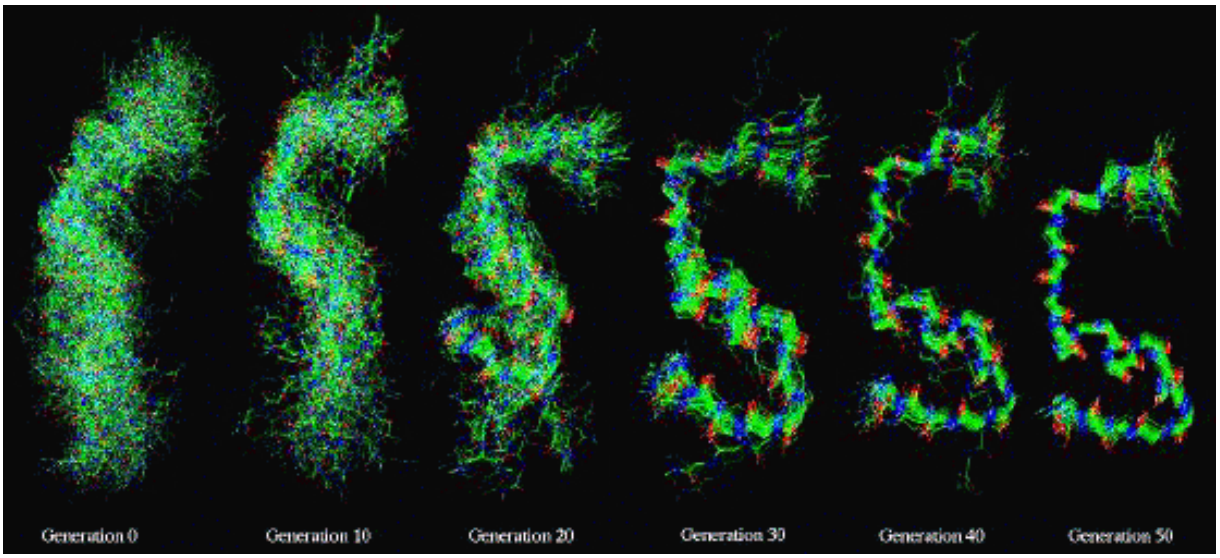

Phys. 72, 259 (2000)

ABSTRACT

Fluorescence resonance energy transfer (FRET) is an electrodynamic process by which energy is transferred from an excited-state donor (D) to a ground-state acceptor (A). Primarily, the efficiency of energy transfer strongly relies on the donor-to-acceptor distance (D – A distance) and the relative orientation of the dipole moments of donor and acceptor (κ^2). Other variables are the spectral overlap between donor emission and acceptor absorption, the rate constant for fluorescence emission of the donor, the fluorescence quantum yield of the donor in absence of acceptor, and the refractive index of the medium. FRET is nonradiative since transfer of energy occurs solely through dipole-dipole coupling between the donor and acceptor dyes. The dependence of the transfer efficiency on the D – A distance makes FRET a powerful technique for the study of biological macromolecules that are conformationally mobile for their activity. Particularly, structural fluctuations, or motions, of a biological macromolecule that results in a distance distribution is studied by using *dynamic FRET*. One such biological macromolecule is the transcription factor p53, whose key function is to prevent uncontrolled cell division in multicellular organisms. Using single-molecule FRET, multiple conformations were detected of full-length human p53 that probably arise from interactions between the N-terminal domain (NTD) and the DNA binding domain of each subunit. In addition, TR-FRET measurements indicated a high propensity of the NTD to form polyproline II structures (Huang *et al*., 2009).

CONTENTS

INTRODUCTION

What is FRET?

FRET, Fluorescence Resonance Energy Transfer, is an electrodynamic process that is utilized as a technique to measure distances between (bio)molecules on a nanometer scale. To do so, these molecules are covalently labeled with an appropriate donor and acceptor molecule. A fluorophore in its electronic excited state (the donor) may transfer its energy to an acceptor in the ground-state. The process occurs when provided that certain conditions are met; a) there must be some spectral overlap between the emission spectrum of the donor and the absorption spectrum of the acceptor; b) the donor must be luminescent; and c) the D – A distance should not be too short (<5 nm) or too large (>200 nm) [2]. The energy transfer is a radiationless process and occurs through resonance coupling of dipoles. See figure 1 below for clarification.

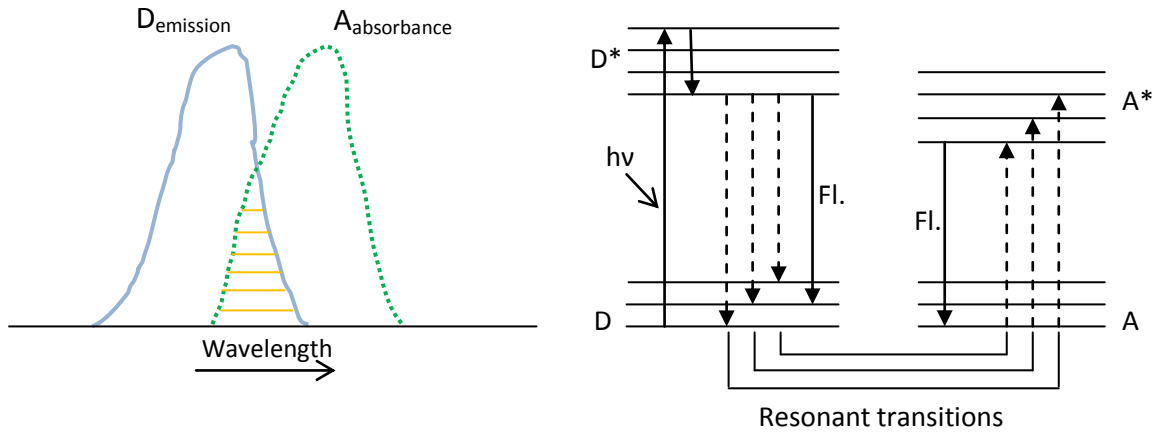

Figure 1: demonstration of the FRET principle showing the energy level diagram (right) to illustrate the mechanism of resonance coupling. This diagram, also named the Jablonski diagram, illustrates the different electronic states of a molecule and the transitions between them. The horizontal lines represent the different vibrational energy levels that exist at each electronic energy level of the fluorophore. In other words, each electronic energy level consists of several vibrational states. The radiative transitions (hv, fluorescence) are shown as solid arrows and the nonradiative transitions are shown as dashed arrows. The excited states of the donor and acceptor are denoted as D* and A* respectively. Left: representation of the spectral overlap between the donor emission and the acceptor absorption [2].

It is important to emphasize that no re-absorption of emitted photons is involved in the energy transfer. The corresponding emission and absorption spectra are one of the necessary conditions in which energy transfer *could* occur. The *actual* energy transfer is based on dipole-dipole interactions or resonant transitions between donor and acceptor. Hence, the acceptor molecule is, though differently depicted in figure 1, not necessarily fluorescent. As long as its dipole moment resonates electro-dynamically to the donor dipole moment. On a much larger scale this process resembles two resonating tuning forks. If one fork is vibrating in a period that it can resonate with another, energy will slowly dissipate from one fork, while the other begins to vibrate.

The transfer efficiency in relation to the Förster distance

The FRET efficiency *E* is the fraction of excited fluorophores that decay to the ground state through the FRET mechanism. Suppose *E* = 50%. This means that upon introducing an acceptor, the excited state donors depopulate at a doubled fluorescence decay rate. The following equation gives the FRET efficiency

$$E = \frac{R_0^{\,6}}{R_0^{\,6} + r^6}$$

where r is the D – A distance and R_0 is the Förster (critical) distance at which 50% of the donor molecules decay by nonradiative energy transfer. That is to say, the D – A distance at which FRET efficiency is 50%. The value of R_0 differs per D – A pair. In ideal cases, the distance measured differs very slightly from the Förster distance.

The equation clearly expresses the distance dependence ($1/r^6$) on the FRET efficiency, which was calculated by Theodor Förster. If the donor and acceptor are in close proximity (r is small), then E will be near unity. A slight deviation of r from R_0 results in a dramatic change in FRET efficiency (Figure 2).

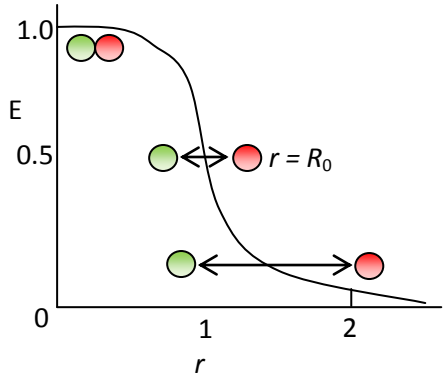

Figure 2: FRET efficiency plotted against the inter-fluorophore distance to illustrate how E depends on R_0.

An important parameter in determining the Förster distance is the orientation factor (κ^2) which describes the relative orientation in space of the dipole moments of the fluorophores. Due to their dynamic nature in most systems, the relative orientation of donor and acceptor is not fixed. In other words, the relative orientation of the dipole moments changes in time. The value of the orientation factor κ^2 (derivation not shown) may range from 0 to 4. Ideally, the dipoles of the donor and acceptor are parallel (κ^2=1). The value of 4 is only obtained when both dipole moments are collinear (along the same line). Generally, the measurement of R_0 is only influenced by 26% if κ^2 ranges from 1 to 4. However, the error in determining the distance gets bigger when the dipoles are oriented perpendicular to each other [1]. If the donor or acceptor undergoes fast isotropic motions the value is averaged to $\kappa^2 = \frac{2}{3}$ which is usually assumed [3].

FRET is widely used as a technique to study biological macromolecules since the Förster distance is usually comparable to the diameter of many proteins and the thickness of biological membranes [3]. In most experimental contexts a donor and acceptor fluorophore are covalently labeled to certain sites of a protein or DNA molecule. Biological activity of these macromolecules results in changes of the D – A distance, *i.e.* conformational changes of a protein result into various distances between the donor and acceptor fluorophore attached to the protein at fixed positions. If the inter-dye distance is very small FRET efficiency will be near 100% and all the energy is transferred to the acceptor.

From steady-state to time-resolved measurements

For studying interactive and dynamical properties of proteins, a typical FRET experiment consists of a certain protein sample solution and a fluorescence measurement system. Commonly, one uses steady-state fluorescence measurements in which the sample is constantly illuminated and the fluorescence emission is recorded. To obtain FRET efficiencies one must record an emission spectrum of the donor in the absence and presence of acceptor (Figure 3).

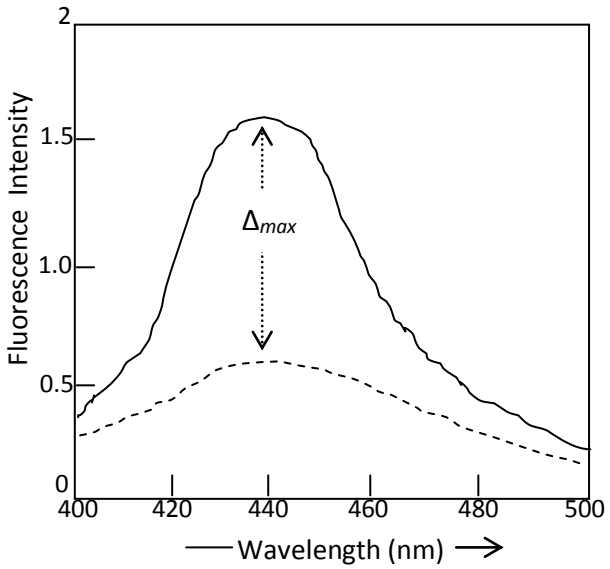

Figure 3: example of a fluorescence emission spectrum using steady-state measurements. (——) donor in absence of the acceptor. (- - - -) donor in presence of the acceptor.

From figure 3 one can easily derive that the fluorescence intensity of the donor decreases in presence of an acceptor. When the FRET efficiency *E* is relatively high, then only a small number of excitation events will contribute to fluorescence and the intensity is lower. In the example above the fluorescence intensity is about 70% quenched upon introducing an acceptor molecule. The degree to which an excitation event gives rise to fluorescence informs about the quantum yield of the donor. The fluorescence quantum yield is the number of emitted photons relative to the number of absorbed photons. The rate of all decay events, radiative (Γ) and nonradiative (k_{nr}) , depopulate the excited-state molecules. The equation below gives the fraction of excited fluorophores that decay through emission, therefore the quantum yield [3].

$$Q = \frac{\Gamma}{\Gamma + \Sigma\, k_{nr}}$$

As can be derived from the equation, the quantum yield is near unity when the nonradiative decay events (k_{nr}) are much slower than the radiative events (Γ) and, hence, $0 \leq Q \leq 1$. The fluorescence quantum yield is calculated by taking the integral of the spectrum (figure 3) and then comparing this value with the spectrum of a fluoropore of which *Q* has been established. The inverse of Γ and the sum of all nonradiative decay events gives the lifetime of the fluorophore.

$$\tau = \frac{1}{\Gamma + \Sigma\, k_{nr}}$$

The lifetime or decay time is a statistical average because fluorescence is a random event. For a large number of fluorophores, some will emit quickly following the excitation event, others will emit at longer times than the lifetime. Only a small fraction emits at $t = \tau$. Hence, the lifetime of a fluorophore is its average time the fluorophore spends in the excited state. When an excited fluorophore returns to the ground state entirely through radiative decay, one speaks of the natural or intrinsic lifetime [3]. The lifetime of most small organic molecules is in the order of 1 – 10 ns. However, values ranging from hundreds of nanoseconds to the microsecond timescale have been found; lanthanides display decay times of 0.5 – 3 ms [3]. Steady-state measurements are inappropriate for the measurement of fluorescence intensity decays. Recall that for steady-state kinetics the sample is illuminated with a *continuous* beam of light. Hence, the data from steady-state measurements is subjected to extensive averaging. For instance, if a protein contains two labeled fluorescent probes with distinct lifetimes this will yield a single steady-state decay time. Spectral overlap between the absorption and emission makes resolution of two separate emission spectra difficult. However, if the sample is exposed to light pulses with a pulse width shorter than the lifetime of the fluorophore, then the lifetime *can* be recovered. For this one uses a high-speed detection system that allows measurements on the nanosecond timescale. This particular procedure is employed by the more complex time-resolved measurements. With these particular measurements, valuable details can be recovered that would have been lost upon averaging the data obtained from steady-state measurements [3].

Time-resolved measurements yield more accurate resolutions of the relative intensity decays resulting from fluorescence quenching. When introducing an acceptor the fluorescence intensity from the donor decreases upon resonance energy transfer. Most time-resolved intensity decays are plotted on a logarithmic scale since this gives a linear function (Figure 4).

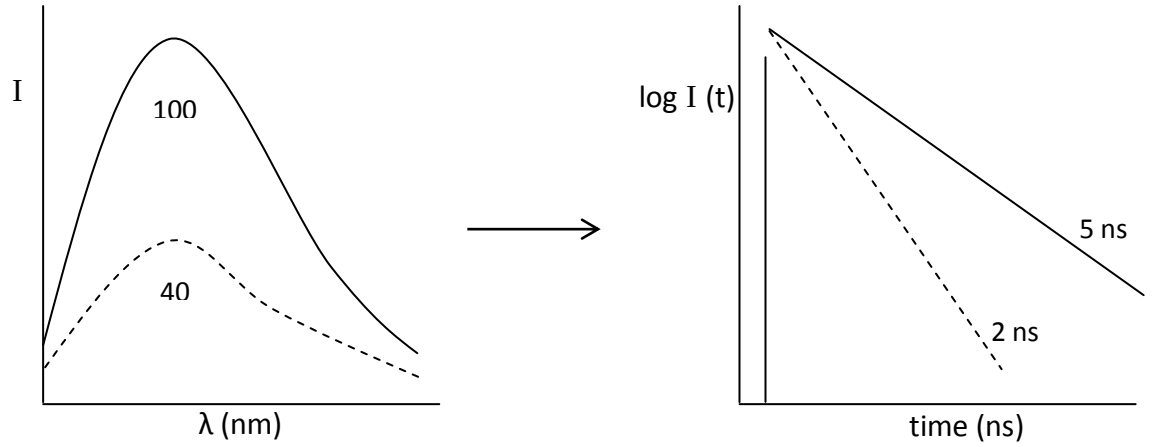

Figure 4: comparison of steady-state intensity decays (left) and time-resolved intensity decays (right). Solid lines represent the intensity decay of the donor without acceptor and dashed lines with acceptor. The numbers in the left plot are the integral values of the curves which represent the fluorescence quantum yield. The vertical bar in the right plot illustrates the excitation-pulse used in time-resolved measurements.

A drop in quantum yield of 60% ($\Delta Q = 60$) is equal to a drop in lifetime of 60% as τ decreases from 5 to 2 ns. The added acceptor has the effect of a quencher because the excited-state donors may now depopulate through another route, that of resonance energy transfer. Therefore a smaller fraction of excitation photons contribute to fluorescence emission and, consequently, the lifetime decreases.

The relative intensity decrease depicted in figure 4 indicates a FRET efficiency of E = 60%, meaning that 60% of the excited-state donors had depopulated through RET.
In ideal cases, the sample displays only one decay time (mono-exponential decay). However, single-tryptophan proteins typically exhibit complex intensity decays due to the distribution of rotamers which are conformational isomers of the same molecule. The indole moiety from tryptophan is known to adopt three rotamers. In addition, the molecular environment of tryptophan strongly influences its intensity decay. In sum, these conditions give reason to fit the observed intensity decays of single-tryptophan proteins to the multiexponential model below [3].

$$I(t) = \sum_i \alpha_i \exp(-t/\tau_i)$$

where the sum of α_i is normalized to unity since the total intensity is not measured. The α_i parameter is called the preexponential factor or amplitude and represents the fraction of fluorophores present at each decay time. For a protein with a single probe displaying a complex intensity decay, it is generally assumed the intrinsic fluorescence decay rate is constant for each molecular environment. Then, the α_i values represent the fraction of molecules in each conformation at t = 0 ns. Usually the α_i values differ with each environment, conformation, of the same molecule. Suppose a single-tryptophan protein reveals three decay times of 1 ns, 5 ns, and 2 ns. These values were obtained, by fitting the observed intensity decays to a triple-exponential decay model

$$I(t) = 0.2 \,.\, e^{-t/1} + 0.5 \,.\, e^{-t/5} + 0.3 \,.\, e^{-t/2}$$

in which the chosen α_i values provide the best fit (plot not shown) to the observed intensity decays. An α_i value of 0.2 means that a 20% fraction of all fluorophore molecules generates a decay time of 1 ns. Now, suppose an acceptor is introduced into the protein. In the next section it will be further revealed what valuable information on protein dynamics can be gained from such an experimental set up.

Dynamic FRET and the averaging problem

In the previous section the fluorescence lifetime dependence on the environment was elucidated to some degree. The local environment of the fluorophore determines to a large extent its decay properties. The emission of some fluorophores, especially tryptophan, are very sensitive to changes in the local environment. If the probe can exist in two environmental states, such as two different conformational states of a protein, then each of these states is assigned to a unique decay time. In fact, a whole ensemble of conformers is usually achieved during folding. With equilibrium unfolding, for instance, a protein is unfolded by gradually changing its solution conditions. As a protein unfolds upon increasing the denaturant concentration, a fluorescent (donor) molecule is exposed to an ensemble of molecular environments. When an acceptor is introduced, the distance between donor and acceptor is influenced by the dynamic behavior of proteins. By using flexible polypeptides a range of donor-to-acceptor distances can be studied. The use of FRET where a typical distance distribution exists is called *dynamic FRET*.

Generally, a protein is labeled with a single donor and acceptor to unique sites. The choice of these two labeling sites depends on the aim of the particular experiment. This may vary from folding studies to interaction studies, *e.g.* protein-protein or protein-DNA interactions. A general procedure of a protein folding study will clarify the concept of a distance distribution.

For a well structured protein, one expects the D – A distance to be well defined since there should be a single conformation. The distance distribution, therefore, displays a sharply defined distance at a specific value of *r*.
Suppose the protein is unfolded to a random coil by gradually adding denaturant. Since the protein has reached a state where random conformations exist (random coil) a wide range of D – A distances is now possible. Instead of a sharply defined distance the distance distribtion now shows a very broad peak that reflects all possible D – A distances in an unfolded protein (figure 5).

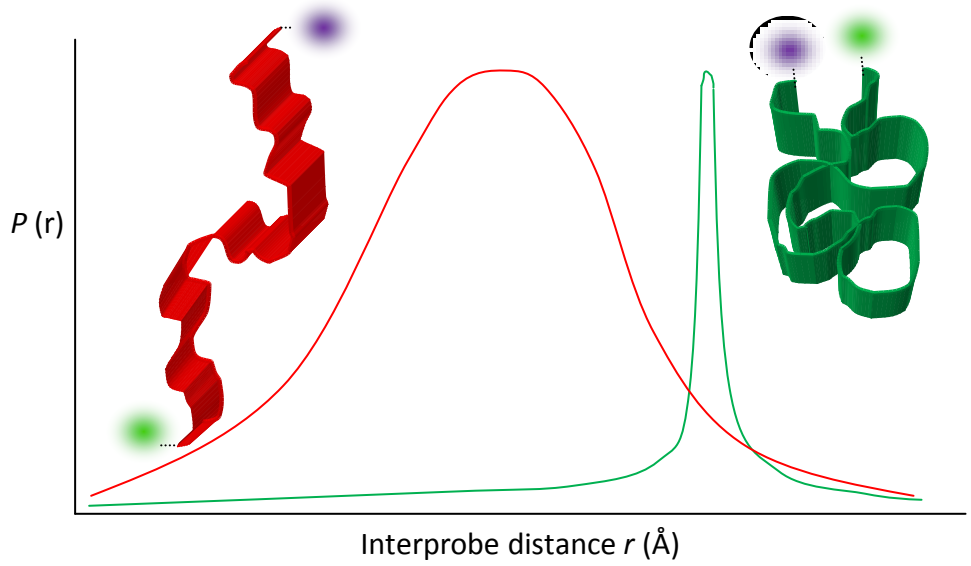

Figure 5: intramolecular distance distributions for D – A pairs in native (—) and denatured (—) proteins. The areas under both curves are normalized to unity to correspond to accord to a single D – A pair per protein. Green and violet spheres represent the labeled fluorescent probes.

As these experiments address the changes in distances *within* a protein, we preferentially speak of intramolecular distance distributions or IDD. A typical distribution is in fact a probability distribution for a whole range of D – A distances (figure 5). In general, it is difficult to determine the actual shape of the distribution from the observed intensity decays. The most appropriate description of the distribution is formed by a Gaussian *P*(r) that determines the weighted average of the donor intensity decays for all D – A pairs with a unique distance *r* [3].
A distance distribution strongly influences the time-resolved decay of the donor (figure 4; right plot). A single D – A distance, as is present in most native proteins, displays a single transfer rate for all donors. In the presence of an acceptor, the decay time of the donor is diminished by the D – A energy transfer rate. On the assumption there is a single distance, the particular distance can be calculated using the relative fluorescence intensity of the donor (figure 4; right plot). This latter measurement gives in fact the transfer efficiency. When R_0 is known the relative fluorescence intensity decays can be used to calculate the D – A distance *r* (equation page 4).
Now, consider the case where a distance distribution exists. A range of distances now exits and thus a range of D – A transfer rates and decay times. Hence, instead of a mono exponential, the donor decay has become multiexponential. This particular change is indicated by curvature in the linear graph from figure 4 (donor intensity decay in the presence of acceptor). The width of the distribution is directly related to the ensemble of protein conformations; a relatively broad distribution indicates a broad ensemble, therefore a relatively loose-packed protein structure [3].

As outlined in the previous section, typical single-probe proteins display decay kinetics that can best be fitted to a multiexponential decay model. This has led to an almost inevitable difficulty concerning averaging processes. Consider the example where a single-tryptophan protein reveals three decay times in a time-resolved measurement (page 7). Each of the α_i values given in the example generate a specific fluorescence intensity decay, *i.e.* 20% of the tryptophan molecules generate a decay time of 1 ns.
Now, suppose an acceptor is introduced into all protein molecules and a single D – A pair for each protein exists. Due to resonance energy transfer the decay times are reduced. Because more than a single decay time had appeared, it is impossible to couple the decreased decay times to their original donor-alone decay times. Suppose, in a measurement, 100% of the tryptophan molecules display a single decay time of 4 ns. When an acceptor is introduced and a decay time of 2 ns is now measured it is certain this decrease came from the decay time of 4 ns. However, in the presence of several decay times distributed according to their α_i values, it remains uncertain which original values (τ donor alone) corresponds to which reduced values (τ donor-acceptor). Therefore, one is forced to average the latter τ values of the donor-alone and D – A system. Thus, the *exact* transfer or FRET efficiency is not resolved. Consequently, this may lead to the calculation of incorrect D – A distances and thus drawing false conclusions about the dynamic nature of the protein in question. The equation below gives the FRET efficiency and illustrates how this averaging problem comes about.

$$E = 1 - \frac{\tau(DA)}{\tau(D)}$$

The nominator gives the decay time of the donor in presence of the acceptor and the denominator the decay time of the donor alone. The transfer efficiency can be obtained from these relative intensity decays when doing time-resolved measurements [3]. If the experiment is done using steady-state measurements one compares the fluorescence intensity of the donor in the absence and presence of the acceptor. The problem arises when it is impossible to recover the original decay time, τ (D), from the decay time of the donor in presence of the acceptor. However, if the lifetimes in both situations are closely spaced, the deviation from averaging the values will be minimal. For example, the donor may displays two decay times of 7 and 6 ns. Then an acceptor is attached to the protein and the decay times have dropped to 4 and 3 ns. Although it is not possible to retrace which decreased decay time corresponds to which original decay time, it is save to average the values and then calculate the transfer efficiency.
A final remark to make is that, besides the conventional ensemble measurements, FRET can also be applied at the single-molecule (SM) level. In a SM-study, one works with highly diluted protein concentrations. Single molecules diffuse through a confocal laser focus that excites the labeled fluorophores. Each pass is followed by a fluorescence burst; a transient emission of photons.
The dominant reason for choosing SM-FRET is to avoid ensemble averaging. Suppose a solution contains two types of fluorophores. The emission spectra of a single molecule in the mixture will be representative of just one type of molecule, and not an average spectrum. However, the signals obtained by individual molecules are relatively weak; a low signal-to-noise ratio. Generally, a combination of ensemble and single-molecule FRET are appropriate for the acquisition of valuable information on structural and dynamical features of biological macromolecules.

Aim of this thesis

As made clear so far, the general aspects of fluorescence resonance energy transfer form the scope of this thesis. Particularly, the aim is to illustrate the potentials of dynamic FRET as a unique tool to study structural dynamics of proteins. In achieving this, the rest of this thesis focuses on the study of the conformational dynamics of the tumor suppressor p53. This study will highlight the potentials of dynamic FRET as well as single-molecule FRET explicitly (Huang *et al*., 2009)[1].

Background

The tumor suppressor protein p53 (protein 53) is a tetrameric, multidomain transcription factor and regulates the cell cycle in multicellular organisms. It is essential for apoptosis, stability of the genome, and inhibition of angiogenesis. Because human p53 (and p53 in general) has been found to exhibit peculiar dynamic behavior it forms an outstanding yet tricky candidate for structural biology studies. Previous data revealed the existence of two folded domains and intrinsically unstructured domains at both termini. The folded domains are comprised of the DNA-binding core domain (CD; residues 94 – 294) and the tetramerization domain (TetD; residues 323 – 360) [4, 5]. The intrinsically disordered N-terminal domain (NTD; residues 1 – 94) and C-terminal domain (CTD; residues 360 – 393) [6, 7] mediate interactions with several proteins for its own regulation. Furthermore, both disordered terminal domains form target sites for posttranslational modifications that modulate the activity of p53. All domains mentioned are summarized in the schematic review below.

Figure 6: structural organization of p53

The aim of the study presented here was to acquire more information on the quaternary structure of p53 than what was achieved before [8]. More information on the disordered structures and domain-domain interactions could not be obtained from conventional techniques, such as X-ray crystallography and NMR spectroscopy. Huang and colleagues relied upon the advantages of ensemble and single-molecule FRET to investigate the inherent conformational heterogeneity present in a single tetrameric p53 molecule. At the same time they highlighted in the consistencies observed between ensemble and single-molecule measurements.

Creating a FRET setup

As the N-terminal domain of human p53 (p53N) is free of cysteine residues these had to be introduced to serve as anchoring sites for fluorescent probes. Several mutants were made, each of which contained two cysteine residues so a range of distances could be measured: p53N(1C-91C); p53N(10C-56C); and p53N(56C-91C). The inserted cysteines were randomly labeled with Alexa Fluor 488 (AF488; FRET donor) and Alexa Fluor 647 (AF647; FRET acceptor). Control experiments using the B-domain of protein A indicated no noticeable effects of random labeling on the SM-FRET efficiency histograms [9].

The choice of Alexa Fluor as fluorescent dyes was not consistent with previously measured intramolecular distances, as is the usual case though. When an (average) intramolecular distance in a protein is known that can reveal valuable information, one commonly chooses a D – A pair with approximately the same Förster critical distance as the measured distance in question. For this study, the investigators chose Alexa Fluor dyes as these were used in a previous similar study and, nevertheless, the single-molecule measurements were based upon this particular study [9]. However, what has been carefully considered were the positions at which the cysteines were introduced as these established the donor-to-acceptor distances to be measured.

The intact full-length peptide chain of p53 (flp53) harbors ten cysteine residues, some of which are (partly) exposed and others are buried. To prevent mislabeling, all of the exposed and partly exposed cysteine residues were mutated to alanine. The buried cysteine residues were used in the

FRET setup as these residues were found to comprise (in part) zinc finger domains and are therefore localized in the DNA binding core domain (C176, C238, and C242). To explore the quaternary structure of flp53 and its potential domain-domain interactions, a series of mutants were made: flp53(56C-229C), flp53(56C-292C), flp53(2C229C), and flp53(2C394C). Note, full-length p53 concerns one monomer of the entire assembly; only one monomer of each tetramer was labeled.
Fluorescent dyes labeled at the N-terminal domain p53NTD (56C-91C)and full-length p53 (56C229C) were used to determine the Förster critical distances (R_0). For the AF488/AF647 pair the R_0 value was approximately 52 Å which allows accurate distance measurements between 42 and 66 Å, corresponding to FRET efficiencies of 0.8 and 0.2 respectively. Another D – A pair (AF546/AF647) was used to measure larger distances. This pair had a R_0 value of approximately 63 Å. Finally, extensive control experiments were done to check for anomalies of the overall structure and DNA-binding abilities of p53 due to the presence of fluorescent dyes (not discussed further).

Using SM-FRET to measure donor-to-acceptor distances in the N-terminal domain of p53
The mutants p53N(10C-56C) and p53N(56C-91C) with AF488/AF647 as donor/acceptor couple displayed a single peak (apart from the 'zero peak') in the SM-FRET efficiency histogram. The peaks of the two mutants were located at a efficiency value of 0.45 and 0.41, respectively. The single peak pattern, or unimodal distribution, proposes a single ensemble of conformations that could be observed in the NTD of p53. Moreover, in a previous study on protein folding it was proved that the "zero" peak in the apparent FRET efficiency histogram was predominantly due to the photobleaching of the AF647 acceptor [9].
No peak was observed of the full-length NTD mutant, p53N(1C-91C), except the zero peak. This suggested the inter-probe distance was too long and the AF546/AF647 couple had to be used since this gives a greater Förster critical distance. This resulted in a peak-shift from a low to high FRET efficiency. The peak-shifts of all mutants, as well as the apparent average distances, are summarized in table 1. The equation $r = (1/E_{peak} - 1)^{1/6} R_0$ was used to calculate the apparent average distances between the fluorescent probes. The distances calculated from the AF546/AF647 system were greater than those calculated from the AF488/AF647 system. The finding of this broad distance distribution confirmed the intrinsic flexibility of the N-terminal domain of p53. Histograms from two mutants are shown in figure 7.

As explained in the section about the Förster critical distance of any particular FRET system, it is desired to measure a transfer efficiency around 50% (Figure 2). A dramatic deviation of r from R_0 results in either a too low or too high FRET efficiency. The mutants p53N(10C-56C) and p53N(56C-91C) gave a FRET efficiency slightly < 0.5 when AF488 was used as donor and slightly > 0.5 when AF546 served as donor. Therefore, the actual distances between the dyes must be between 54 and 58 Å for p53N(10C-56C) and between 56 and 62 Å for the p53N(56C-91C) mutant. A FRET efficiency of only 0.25 was measured for the p53N(1C-91C), assuming the actual distance might be > 76 Å**.**

Table 1: FRET efficiencies and distances between residues in the NTD of p53

Observable	**p53N(10C-56C)**	**p53N(56C-91C)**	**p53N(1C-91C)**
$E_{488\text{-}647}$	0.45	0.40	NA
$E_{546\text{-}647}$	0.61	0.53	0.25
$R_{488\text{-}647}$ (Å)	54	56	NA
$R_{546\text{-}647}$ (Å)	58	62	76

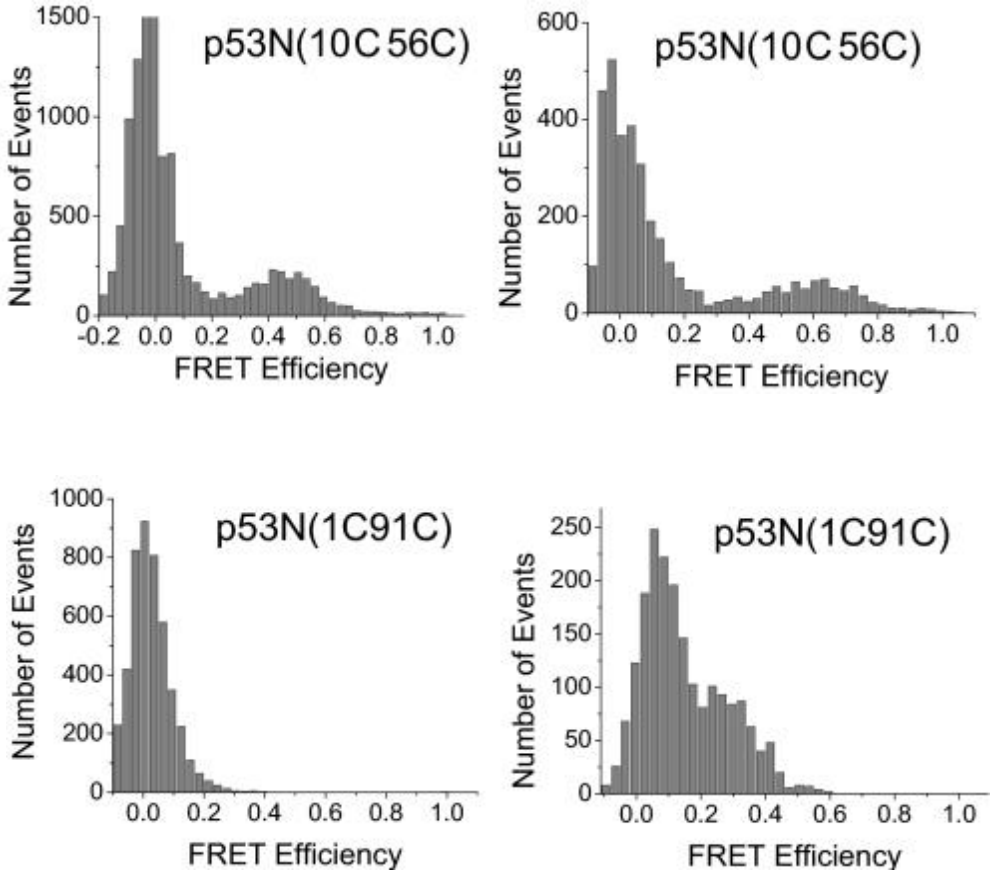

Figure 7: single-molecule FRET histogram for isolated NTD with dyes labeled at positions 1, 10, 56, and 91. Switching from the AF488/AF647 pair (left) to the AF546/AF647 pair (right) resulted in a peak-shift to higher FRET frequencies. Note that every histogram contains the "zero" peak. The number of events on the vertical axis represents the number of detected photons per fluorescence burst [1].

Using ensemble-FRET to measure donor-to-acceptor distances in the N-terminal domain of p53

To demonstrate the consistencies between single-molecule and ensemble-FRET, a similar experiment was set up using the latter type of FRET measurement. A series of short peptides was synthesized to obtain average distances and a distance distribution between residues in the NTD of p53:
residues 1-17 (p53N1-17), residues 14-30 (p53N14-30), residues 62-78 (p53N62-78), and residues 74-92 (p53N74-92). All peptides were end-labeled with donor and acceptor molecules. Time-resolved intensity decays of the donor were obtained in the presence and absence of acceptor. The distance distribution was recovered by fitting the fluorescence data of the donor *with* acceptor numerically to a Gaussian distribution (figure 8).

As depicted, all synthetic peptides displayed rather broad end-to-end distance distributions, suggesting they are relatively flexible and thus confirming the assumption that NTD is intrinsically unstructured. The distributions belonging to p53N14-30, p53N62-78, and p53N74-94 have similar widths and heights. This is probably due to their shared tendency to form helical secondary structures, *i.e.* α-helix like structures [11, 12]. Although circular dichroism spectra (not shown) revealed a clear polyproline II (PPII) structure for p53N74-92 only, the existence of residual secondary structures in the other three peptides was not excluded.

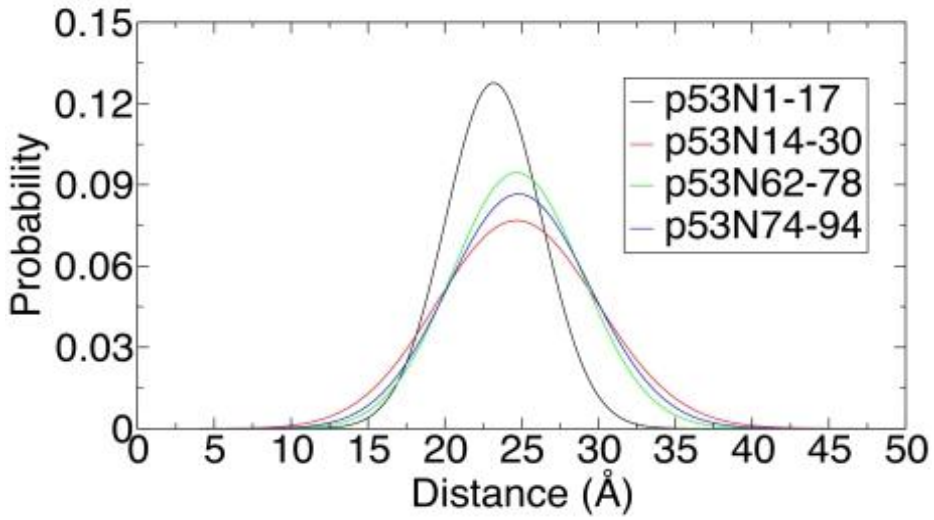

Figure 8: distance distributions for end-to-end distances of synthetic peptides truncated from the N-terminal domain of p53 [1].

The peptide p53N1-17 peaked at smaller mean value and gave a relatively narrow distance distribution. This suggests the peptide consists of less flexible residues making it more rigid overall. One such residue is proline. Despite the broad distance distributions that supported the notion of a flexible NTD, all four peptides gave very small intramolecular diffusion coefficients. This is most likely due to the strong sequence dependence of peptide flexibility, *i.e.* propensity to form helical secondary structures and the presence of proline residues. The diffusion coefficients and other parameters are listed in table 2.

Table 2: parameters of the end-to-end distance distributions for synthetic peptides from the NTD of p53

Parameter	p53N1-17	p53N14-30	p53N62-78	P53N74-92
Mean (Å)	22.3	22.3	23.2	23.0
Standard deviation (Å)	3.2	5.4	4.4	4.8
Diffusion coefficient ($Å^2$/ns)	0.0	0.0	0.4	0.6
X^2 *	1.24	1.28	1.48	1.24

*X^2 is the goodness-of-fit parameter. A value near unity indicates a good fit between observed and hypothetical data.

The dynamic behavior of monomeric p53

The lack of the tetramerization domain (TetD) and the unstructured C terminus gives reason to study p53 in its monomeric state. To do so, the NTD plus core domain (p53NCD; residues 1-292) was subjected to single-molecule FRET measurements. Besides the zero peak, a single broad peak was observed from the FRET efficiency histogram of the mutants p53NCD(56C-229C) and p53NCD(56C-292C). Peak efficiencies and apparent average distances of both mutants are listed in table 3. The histograms are given in figure 9.

Table 3: FRET efficiencies and distances between residues in p53NCD

Observable	p53NCD(56C-229C)	p53NCD(56C-292C)
$E_{488\text{-}647}$	0.63	0.60
$E_{546\text{-}647}$	0.77	0.70
$R_{488\text{-}647}$ (Å)*	48	49
$R_{546\text{-}647}$ (Å)	52	55

* Standard deviations for these values are 2 Å for both mutants

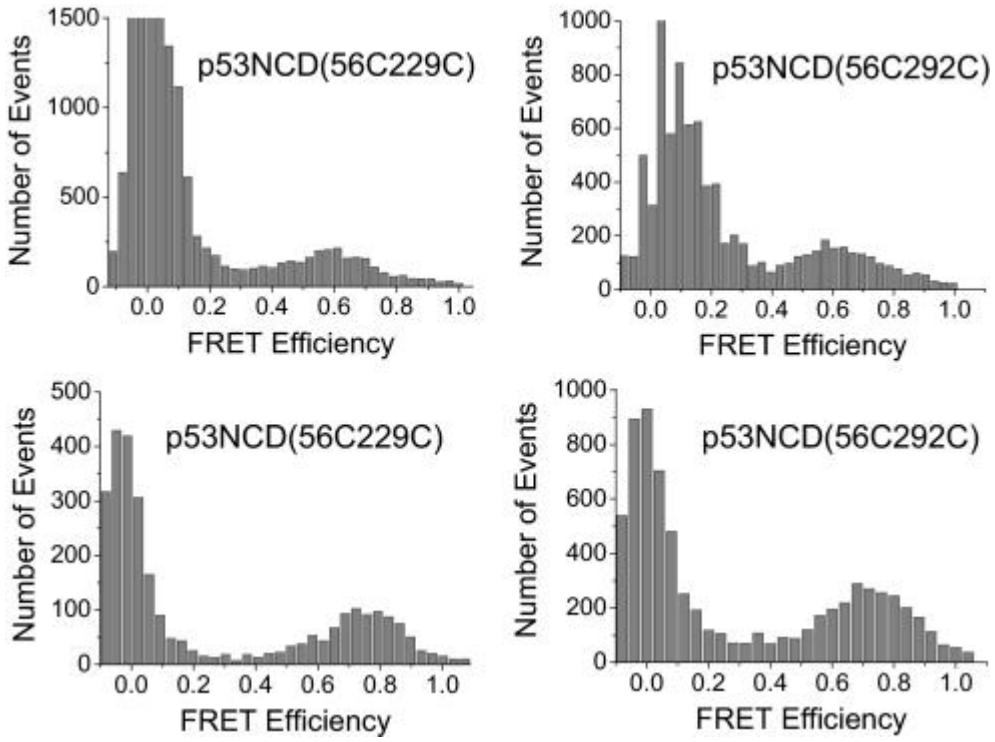

Figure 9: single-molecule FRET histograms for p53NCD mutants with dyes labeled as shown. Upper panel: use of the AF488/AF647 pair. Lower panel: use of the AF546/AF647 pair [1].

Similar to the observations from SM-FRET data of isolated NTD, a peak-shift to larger apparent distances occurred. As mentioned before, a minimal deviation from the Förster critical distance gives reason to regard these particular apparent average distances close to the actual mean distances.
The observation of smaller apparent average distances between residues in p53NCD than measured in the isolated NTD was quite remarkable. This finding clearly indicated a domain-domain interaction between the NTD and CD; without this interaction the average inter-probe distance in isolated NTD is expected to be smaller than that in p53NCD. Because the NTD is extended and highly flexible in solution, a dynamic two-state equilibrium might exists; free NTD and associated with CD.

Several explanations are possible for the appearance of a single peak in the SM-FRET efficiency histogram. One of them is a rapid exchange (< 1 ms^{-1}) of multiple conformational ensembles. This exchange would not be resolvable on single-molecule time scale, observing a weighted average instead (broad peak).

The quaternary structure of full-length p53 and Domain-Domain interactions

Recall from the section *Creating a FRET setup* that several mutants were prepared to explore the quaternary structure of full-length p53 and probe possible domain-domain interactions. Only one subunit of the tetramer was labeled with dyes at a time.

Single-molecule FRET measurements for flp53(2C-229C) did not result into any peak between FRET efficiencies 0.2 and 1 when AF488/AF647 was used. This suggested that the N-terminus of the NTD and the CD are too distant in respect to each other. The lack of peaks was also found for flp53(2C-394C) when either AF488 or AF546 served as donor. Therefore, the distance between both termini of the full-length protein was at least > 80 Å. With these observations it was concluded no interactions between the N and C termini within the same monomer could exist. To look for possible interactions between the N and C termini of *different* monomers in the same tetramer, another experiment was designed in which bulk measurements were set up to maintain labeled p53 in tetrameric states. The FRET system established for every monomer consisted of C2-labeled AF488 as donor and ReAsH as acceptor labeled to the C terminus. The Förster critical distance calculated for this setup was 59 Å. Steady-state fluorescence intensity measurements yield a FRET efficiency of 0.04 that corresponded to an apparent average distance of 100 ± 20 Å. The finding of this rather large distance excluded the possibility of associations between N and C termini among different monomers in the same tetramer. This FRET result is verified by a previous finding where a SAXS model (Small Angle X ray Scatters) of p53 was used [8], but is inconsistent with cryoelecton microscopy results [10].

Different results were obtained when the dynamics of different regions of flp53 were explored. The SM-FRET histograms of the mutants flp53(56C-229C) and flp53(56C-292C) revealed multiple peaks with broad distributions, implying the existence of multiple conformations that interconvert in > 1 ms. It was experimentally excluded that the multiple conformations could be assigned to FRET between different monomers within the same tetramer by maintaining the concentrations of labeled and unlabeled protein to ~100 pM and ~1 µM, respectively. The SM-FRET histograms obtained from measurements of full-length p53 differed substantially from those of p53NCD, even though the labeling sites were equal (56C-229C and 56C-292C). This implied that in context of the tetramerization domain (TetD) and the C-terminal domain (CTD), the domains are differently organized.

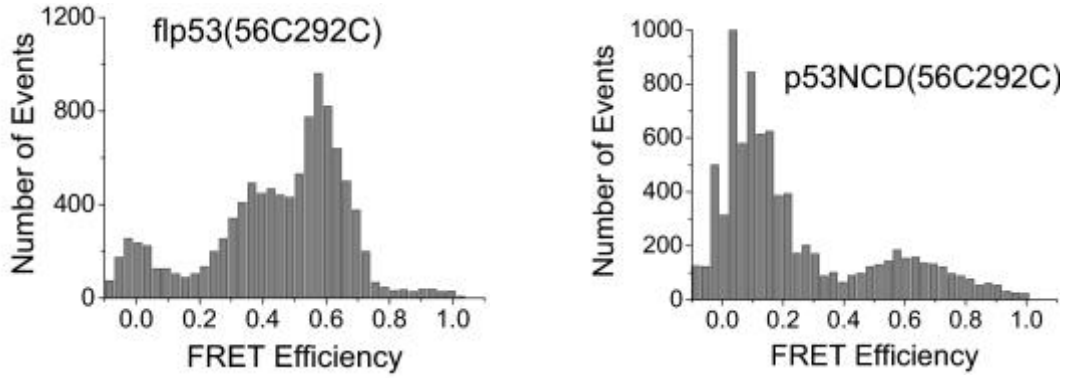

Figure 10: SM-FRET histograms for p53NCD and flp53 with AF488/AF647 labeled at positions as shown [1].

Comparison of the histograms obtained from p53NCD and flp53 learns that tetramerization events influence the relative position of the NTD and CD domains substantially (Figure 10) and so allows the two domains to associate. Due to the flexible and extended nature of the NTD, it is likely it binds to CD domains from other monomers within the same tetramer besides the CD from the same monomer. If, for instance, the NTD binds differentially to the four CD domains within the same tetramer, then four different conformations with different distances are expected in the quaternary structure (Figure 11). Moreover, this confirmation distribution may reflect the multiple peaks observed in the SM-FRET histogram.

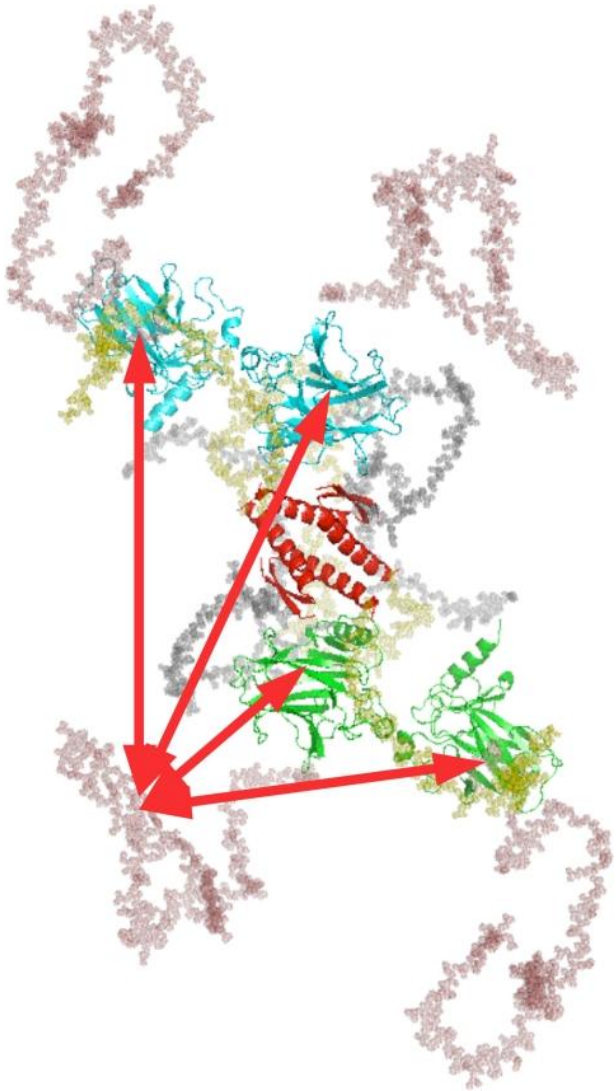

Figure 11: schematic SAXS model of the quaternary structure of full-length p53. (salmon) the NTD domain; (green/cyan) the DNA binding CD domains; (red) TetD domain; (yellow) C termini. Linkers are positioned in the centre and gray colored. The four potential NTD-CD interactions are represented by red arrows [1].

Control experiments were performed to exclude the possibility that the multiple peaks in SM-FRET histograms were caused by protein aggregation. Therefore the diffusion time of the p53 mutants were measured by using Fluorescence Correlation Spectroscopy (FCS). No abnormally slow diffusing proteins were detected which would be the case if protein aggregation occurred. In addition, time-resolved fluorescence anisotropy experiments excluded the existence of restricted fluorophores. Concluding, the multiple peaks in the histogram *did* arise from subpopulations of conformers.

CONCLUDING REMARKS

All data reported in this thesis clearly outline the potentials of dynamic FRET to study conformational dynamics of proteins. Single-molecule and ensemble(time-resolved) FRET measurements on the N-terminal domain of p53 revealed a broad distance distribution and a large apparent average distance, supporting the notion that isolated NTD is extended and flexible. Conversely, mean end-to-end distances obtained from ensemble FRET measurements on synthetic NTD-peptides implied the formation of compact helical secondary structure elements. The tendency of these short peptides to form polyproline II structures was supported by relatively small intramolecular diffusion coefficients. SM-FRET histograms for monomeric p53 showed an interdye apparent average distance that was smaller than observed from analyses of the isolated NTD. This made an interaction between the NTD and CD evident. However, the histograms of full-length p53 pointed out a different organization of these domains in respect to each other. The missing piece for this little conundrum was the presence of the tetramerization and C-terminal domain. The relative positions of the NTD and CD were strongly influenced by TetD and CTD. Finally, from the same analyses it appeared that the N and C termini of flp53 are very distant from one another and multiple conformations exist that interconvert in > 1 ms.

Overall, the data obtained from the FRET studies performed do reply to previous structural data on human full-length p53. A structural model of flp53 from a previous SAXS experiment already excluded the possibility of interactions between the N and C termini of different monomers. This was echoed by the interdye distances found in bulk FRET measurements. However, the SAXS experiments did not confirm the association between the NTD and the CD as these experiments localized only the quaternary structures of the folded domains. From both SAXS and FRET experiments it was found that the NTD has a very extended conformation irrespective of the presence of CD. Because of that, weak interdomain coupling between the NTD and CD was suggested. In the contrary to the FRET results, previous NMR experiments did not suggest an altered structure of CD upon tetramerization events [13]. TetD ensures that p53 maintains a loosely packed set of subunits so that the NTD of each subunit is accessible to the CD of other subunits or monomers. This dynamic behavior results in an ensemble of conformers which, at its turn, is reflected by the appearance of multiple peaks in the FRET efficiency histograms (Figure 10). These weak interactions between NTD and CD could not be directly detected by the previous NMR experiments [13]. The requirements of NMR, high protein concentration and solubility, may hinder the achievement of the same results.

In my opinion, the finding of flexible yet compact synthetic peptides does not make a very significant contribution to the examination of the structure of the NTD in isolation. As far as I am concerned, it can be concluded that the proline residue content of the NTD restricts its flexibility to a certain degree. Overall, the domain is still highly flexible which was indicated by the experiments performed. This intrinsic flexibility makes the domain able to adopt multiple conformations and associate with other domains/proteins. To find a possible dynamic two-state equilibrium between free NTD and bound to CD, I would suggest to perform time-resolved FRET studies (ensemble level) instead of SM-FRET. As former measurements are performed on the nanosecond timescale, it should be possible to track a dynamic equilibrium between conformations that exchange faster than 1 ms^{-1}. Another route to further information about the dynamic and structural properties of p53, is to focus more on the functional context. A protein that contains structurally undefined and extended domains is one that communicates to other proteins, *i.e.* transcription factors, to trigger crucial cellular actions. The tumor suppressor p53 is well known for its meditative role in genome integrity and mitotic division. A FRET system that allows for measurements of *inter*molecular distances may, secondarily though, provide information about the structural and dynamic features of human p53. For instance, the interaction between a DNA molecule and the CD.

LITERATURE

1. Huang F, Rajagopalan S, Settanni G, Marsh RJ, Armoogum DA, Nicolaou N, Bain AJ, Lerner E, Haas E, Ying L, and Fersht AR (**2009**) *Multiple conformations of full-length p53 detected with single-molecule fluorescence resonance energy transfer*. *PNAS*, **106,** no. 49, 20758-20763
2. Haas E, (**2005**) *The Study of Protein Folding and Dynamics by Determination of Intramolecular Distance Distributions and Their Fluctuations Using Ensemble and Single-Molecule FRET Measurements. ChemPhysChem*, **6**, 858-870
3. Lakowicz, Joseph R (**1999**) *Principles of Fluorescence Spectroscopy*, 2nd edition. New York, *Kluwer Academic / Plenum Publishers*, chp. 1, 4, 13-14.
4. Clore GM, et al. (**1995**) *Refined solution structure of the oligomerization domain of the tumor suppressor p53*. *Nat Struct Biol*, **2**, 321-333.
5. Cho Y, Gorina S, Jeffrey PD, Pavletich NP (**1994**) *Crystal structure of a p53 tumor suppressor-DNA complex: Understanding tumorigenic mutations*. *Science*, **265**, 346-355.
6. Dawson R, et al. (**2003**) *The N-terminal domain of p53 is natively unfolded*. *J Mol Biol*, **332**, 1131-1141.
7. Müller-Tiermann BF, Halazonetis TD, Elting JJ (**1998**) *Identification of an additional negative regulatory region for p53 sequence-specific DNA binding. Proc Natl Acad Sci USA*, **95**, 6079-6084.
8. Tidow H, et al. (**2007**) *Quaternary structure of tumor suppressor p53 and a specific p53-DNA complex. Proc Natl Acad Sci USA*, **104**, 12324-12329
9. Huang F, Sato S, Sharpe TD, Ying LM, Fersht AR (**2007**) *Distinguishing between cooperative and unimodal downhill protein folding*. *Proc Natl Acad Sci USA,* **104**, 123-127.
10. Okorokov AL, et al. (**2006**) *The structure of p53 tumor suppressor protein reveals the basis for its functional plasticity. EMBO J*, **25**, 5191-5200
11. Wells M, et al. (**2008**) *Structure of tumor suppressor p53 and its intrinsically disordered N-terminal transactivation domain*. *Proc Natl Acad Sci USA,* **105**, 5762-5767
12. Kussie PH, et al. (**1996**) *Structure of the MDM2 oncoprotein bound to the p53 tumor suppressor transactivation domain. Science*, **274**, 948-953.
13. Veprintsev DB, et al. (**2006**) Core domain interactions in full-length p53 in solution. *Proc Natl Acad Sci USA,* **103**, 2115-2119.

Dankbetuiging:
Ik wil mijn moeder bedanken voor haar engelengeduld.